Multi-axis vibration isolation using different active techniques of frequency reduction

Article *in* Journal of Vibration and Control · April 2011

DOI: 10.1177/1077546310379085

2 authors:

Ahmed Mohammed Abu Hanieh
Birzeit University
30 PUBLICATIONS **229** CITATIONS
SEE PROFILE

A. Preumont
Université Libre de Bruxelles
246 PUBLICATIONS **3,323** CITATIONS
SEE PROFILE

Article

Journal of Vibration and Control
17(5) 759–768

DOI: 10.1177/1077546310379085
jvc.sagepub.com

Multi-axis vibration isolation using different active techniques of frequency reduction

Ahmed Abu Hanieh[1] and Andre Preumont[2]

Abstract

This paper demonstrates a new idea for vibration isolation. Two different techniques of frequency reduction are presented here; the first technique depends on using an active embedded control system with proportional plus integral compensator to reduce the stiffness and corner frequency of the isolator in an active state while keeping high rigidity in a passive state. This type of isolation has proven the ability to reduce the frequency modes to about 50% of the natural frequencies in a passive state. The second technique is based on using phase lead and lag compensators on the unity gain points of the open-loop transfer function. This document will concentrate on single axis isolation although the mentioned isolator can be used as one active leg (strut) in six-axis isolators (Stewart platforms). The experimental results show as well as the simulation ones that these frequency reduction techniques have high performance on the discussed single-axis systems which makes it promising to be applied on multi-axis systems.

Keywords

Active control, frequency reduction, Stewart platform, vibration isolation

Date received: 30 July 2009; accepted: 30 June 2010

1. Introduction

Vibration isolation is becoming more and more stringent as the mechatronic systems are advancing and developing in space and ground applications. In order to obtain high performance from the vibration isolator, the corner frequency should be as low as possible (Rahman et.al., 1994; Preumont, 2002; Abu Hanieh, 2003). This leads the researchers to reduce the frequency by the following ways:

- increase the mass of the equipment needed to be isolated or to reduce the stiffness to have soft isolation mounts either in single or two stages (Nelson, 1991).
- using a hybrid, soft and stiff mounts, with velocity feedback using phase lag and phase lead compensators on the unity gain points (TMC, 2002).
- using totally stiff mount isolator with proportional plus integral feedback compensator.

Increasing the mass or inertia is problematic specifically in space applications because of the limitations on the weights can be transported to space (Karnopp and Trikha, 1969; Kaplow and Velman, 1980). On the other hand, reducing the mount stiffness leads to difficulties in stability of the systems under normal loads in ground applications and ground tests. This paper will present a stiff mount that can be used for the purpose of vibration isolation. This stiff mount can be softened in active ways by using a simple proportional plus integral (PI) compensator. This stiff mount isolator can be used as the active strut (leg) of six-axis Stewart platform interface with piezoelectric actuators to reduce the stiffness

[1]Mechanical Engineering Department, Birzeit University, Birzeit, Palestine.
[2]Service des Constructions Mecaniques et Robotique, Universite Libre de Bruxelles, Bruxelles, Belgium.

Corresponding author:
Ahmed Abu Hanieh, Mechanical Engineering Department, Birzeit University, Birzeit, Palestine
Email: ahanieh@birzeit.edu

and corner frequency of the interface in active mode while keeping high stiffness and rigidity in passive mode (Abu Hanieh, 2003). The first part of this paper will present the main objectives of vibration isolation and some previous efforts in soft and stiff isolation mounts. The theory, design and control of the suggested isolator will be demonstrated in the next part. More concentration will be on simulation results for the system. Experimental results on single and two degrees-of-freedom systems using the idea of frequency variation will be shown in the last part.

Finally, conclusions and future work will be discussed at the end of the paper.

2. Single axis isolator using a piezo stack and intermediate passive mount

Several previous works have been invented to reduce the frequency of the isolation system using piezoelectric actuators. A single-axis vibration isolation system (Quiet pier) has been invented by the Technical Manufacturing Corporation (TMC) to solve the problem of the high corner frequency when using a piezoelectric actuator (TMC, 2002). This system (in Figure 1) consists of a piezoelectric actuator represented by its extension δ and stiffness k, a payload mass m_1 and an intermediate passive mount. The intermediate mount consists of a mass M and an elastomer with a stiffness k_1 and a damping factor c_1. The isolator frequency formed by the stiffness of the actuator k and the intermediate mass M is equal to 1000 Hz. The passive elastomer (represented by the spring k_1 and the dashpot c_1) forms a new resonance with the payload mass m_1 equals to 20 Hz. The two stiffness values, k and k_1 are in series; this results in having the corner frequency of the system corresponding to the lower stiffness k_1. A geophone velocity sensor is installed at the intermediate mass M. The active control strategy is based on feeding the signal of the geophone back to the piezoelectric actuator after being properly filtered and amplified. This inertial feedback leads to quiet the intermediate mass M which results in isolating the motion x_{c1} of the payload mass m_1 from the seismic disturbance x_d. The system can be represented in Laplace transform by the following equations of motion:

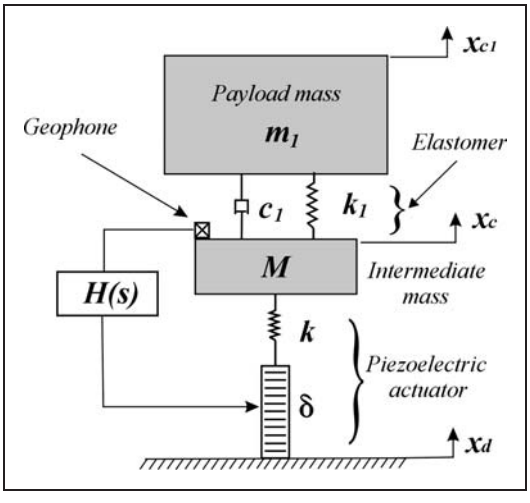

Figure 1. TMC single axis isolator using intermediate soft mount.

The intermediate mass:

$$Ms^2x_c = k(x_d - x_c + \delta) - k_1(x_c - x_{c1}) - c_1s(x_c - x_{c1}) \quad (1)$$

The payload mass:

$$m_1s^2x_{c1} = k_1(x_c - x_{c1}) + c_1s(x_c - x_{c1}) \quad (2)$$

Figure 2 shows the open-loop frequency response function (FRF) between the voltage input to the actuator and the velocity measured by the geophone. The gain (magnitude) of the open-loop transfer function climbs at 40 dB/decade then levels at 40 dB when it reaches to 4.5 Hz at the resonance frequency of the geophone. The geophone acts as a second order high-pass filter that cuts the signals off below 4.5 Hz. The high frequency attenuation is achieved by locating a low-pass filter at 300 Hz (before the resonance of the piezoelectric actuator).

A lag compensator is placed near the low frequency unity gain point (at 0.2 Hz), and a lead compensator is placed near the high frequency unity gain point (at 350 Hz). The advantage of adding this lag-lead compensation is to reduce the amplifications (overshoots) that appear at the unity gain points when the loop is closed. Figure 3 shows the transmissibility FRF between the seismic disturbance displacement x_d and the sensitive payload displacement x_{c1}. The overshoots caused by inertial feedback can be seen clearly on the two unity gain points of the closed-loop FRF. Using a phase lag compensator near the low unity gain frequency reduced the overshoot which means better transient response and lower settling time.

Similarly, using a phase lead compensator near the upper unity gain frequency could increase the phase margin which improves the stability conditions of the system. One can see clearly that despite using a hard piezoelectric actuator, the passive vibration isolation occurs here near the low frequency resonance of the passive mount (20 Hz). Moreover, the closed-loop active vibration isolation occurs much lower than that (at 0.2 Hz) leading the system to have a high isolation performance for a wide band of disturbances.

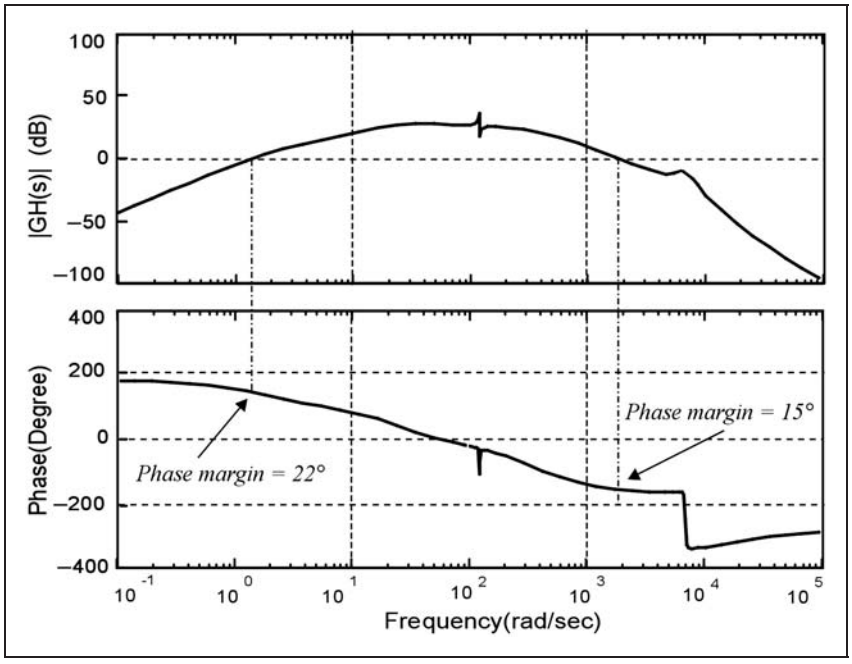

Figure 2. Open-loop FRF of TMC single axis isolator.

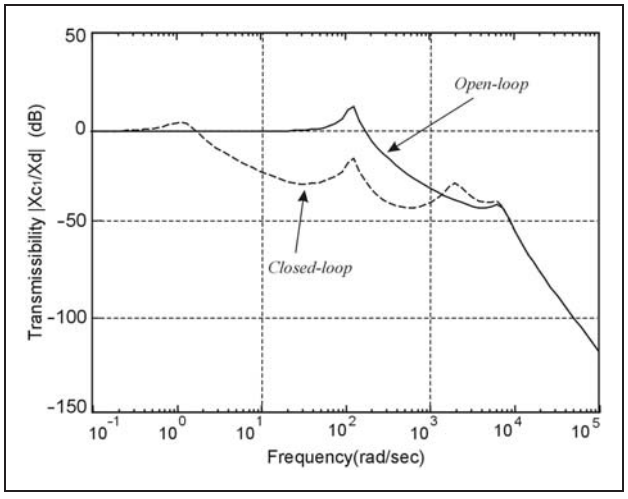

Figure 3. Transmissibility FRF of TMC single axis isolator.

3. Single axis piezoelectric isolator using PI controller

Consider the schematic drawing shown in Figure 4. This figure represents a vibration isolation interface with the disturbance source (mass m), the sensitive payload (mass M), a force sensor F and a piezoelectric actuator represented by its stiffness k and extension δ. PI feedback controller is used here to reduce the corner frequency and improve the response. This system can be used as an active strut for the previously mentioned Stewart platform. As an application for the frequency

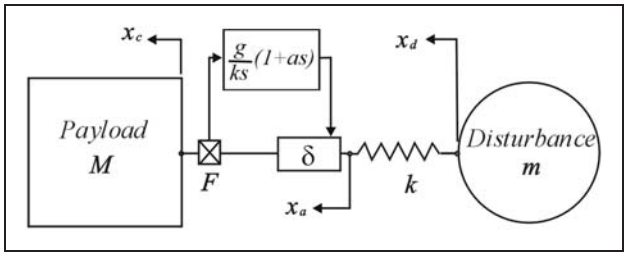

Figure 4. Single axis piezoelectric isolator with PI feedback.

reduction, one can imagine adaptive structures that can change their resonance frequency instantaneously to avoid being excited when the excitation frequency approaches a resonance.

The active feedback controller is applied by acquiring the signal measured by the force sensor and feeding it back to the piezoelectric actuator after being filtered and compensated with PI compensator. The PI controller $\left[\frac{g}{ks}(1+as)\right]$ consists of an integration controller with a gain g plus a proportional controller with a gain ga, the gain is normalized with the stiffness k. The force on the payload is measured and fed back to the actuator after being processed by the PI controller. The governing equation of motion for the system in Laplace transform is:

$$Ms^2x_c = -ms^2x_d = k(x_d - x_a) = F \tag{3}$$

and

$$\delta = x_c - x_a \tag{4}$$

The open-loop FRF between the extension of the piezoelectric stack in the piezoelectric actuator δ and the output of the force sensor F reads:

$$\frac{F}{\delta} = k\frac{Mms^2}{Mms^2 + k(M+m)} \tag{5}$$

Applying a force feedback control strategy using a proportional plus integral compensator, the control law reads:

$$\delta = \frac{g}{ks}(1+as)F \tag{6}$$

Here ga is the proportional gain and g is the integral gain. The root locus for the closed-loop poles of this system is shown in Figure 5; it shows that increasing the loop gain decreases the frequency of the closed-loop poles. If the proportional term is used alone, the poles will move on the imaginary axis towards the origin but this means the risk of destabilizing the system at any instant. The use of the integral controller here pushes these poles deeper to the left half plane increasing the stability.

From the analytical calculation, the intermediate displacement x_a is:

$$x_a = \frac{sx_c + g(as+1)x_d}{s + g(as+1)} \tag{7}$$

From the foregoing equations, one can calculate the transmissibility FRF between the disturbance displacement and the payload displacement, which is equal to:

$$\frac{x_c}{x_d} = \frac{1}{s^2\left[(1+ga)/\omega_n^2\right] + s\left[g/\omega_n^2\right] + 1} \tag{8}$$

Where ω_n is the natural frequency of the system. This implies that the corner frequency ω_c of the system is determined by the proportional gain of the compensator:

$$\frac{1}{\omega_c^2} = \frac{1+ga}{\omega_n^2} \tag{9}$$

The damping of the system is determined by the gain g of the compensator

$$\frac{g}{\omega_n^2} = \frac{2\xi}{\omega_c} \tag{10}$$

If ω_n is much larger than ω_c then

$$\begin{aligned} \frac{\omega_n^2}{\omega_c^2} &\approx ga \\ \frac{ga}{k} &= \frac{1}{M\omega_c^2} = \frac{1}{k^*} \end{aligned} \tag{11}$$

Here $(1/k^*)$ is the closed-loop flexibility of the system and is proportional to the gain. From the foregoing analysis, one can see that the closed-loop stiffness of the system is inversely proportional to the control gain; in other words, if one increases the proportional gain, the stiffness is reduced.

4. Simulation results

The system shown in Figure 4 has been simulated using Matlab software. The simulation was based on the previous analysis of the system taking the mass m as 1.1 kg, the mass M as 1.7 kg and the stiffness of the piezoelectric actuator k as $1*10^7$ N/m. Figure 6 depicts the root locus prediction that the poles should follow when the

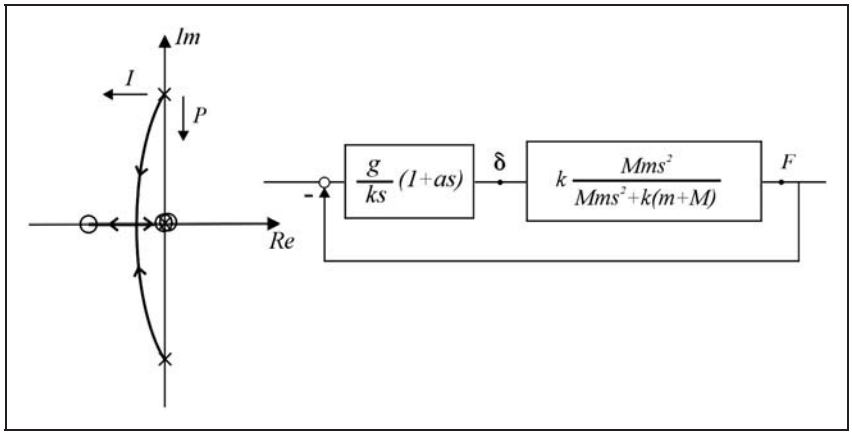

Figure 5. Root locus of single axis piezoelectric isolator with PI feedback.

control loop is closed. The root locus shows that the poles will remain in the left hand side of the s-plane which means that the system is unconditionally stable unless a high-pass filter is added to the system which restricts the control performance. On the other hand, the loop of the plot is not moving in a circular shape which means that when we increase the gain of the controller the distance between the pole and the origin will be shorter leading to slow down the poles or to reduce the frequency of the corresponding mode.

Theoretically, the poles will move till reaching critical damping but in real time work this is impossible as will be shown in the experimental verification part. Figure 7 shows the transmissibility FRF (x_c/x_d) before and after stiffness reduction using PI controller.

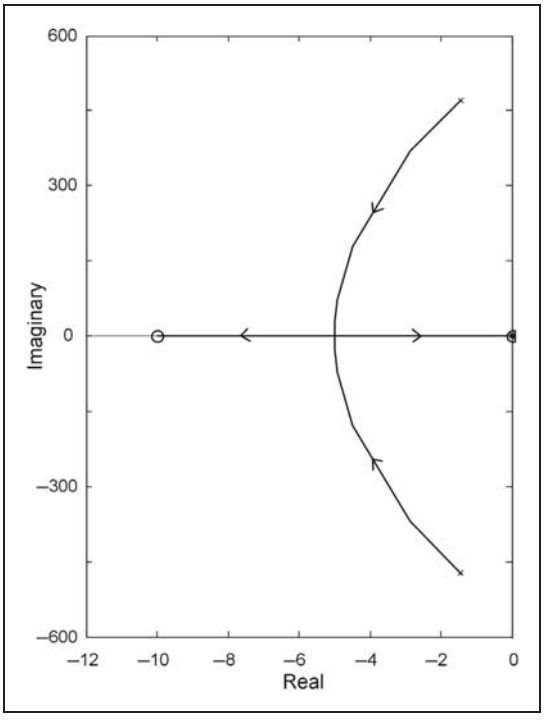

Figure 6. Root locus prediction.

5. Experimental verification

The experimental set-up shown in Figure 8 has been built and tested to verify the principle of using PI feedback control technique for the purpose of active vibration isolation by frequency reduction in a manner similar to the analysis of the set-up discussed theoretically in the previous section. The experimental set-up shown in Figure 8 consists of two masses (1.1 and 1.7 kg) connected to each other by an active member. The active member consists of a Cedrat APA50 piezoelectric actuator, a B&K 8200 piezoelectric force sensor with charge output and two flexible joints to avoid the side effect of the lateral modes of the system by decoupling these modes mechanically from the axial studied mode.

In order to apply the feedback control technique, the signal produced by the force sensor, attached to the payload mass (1.7 kg), is amplified and conditioned using a Nexus charge amplifier and converted into

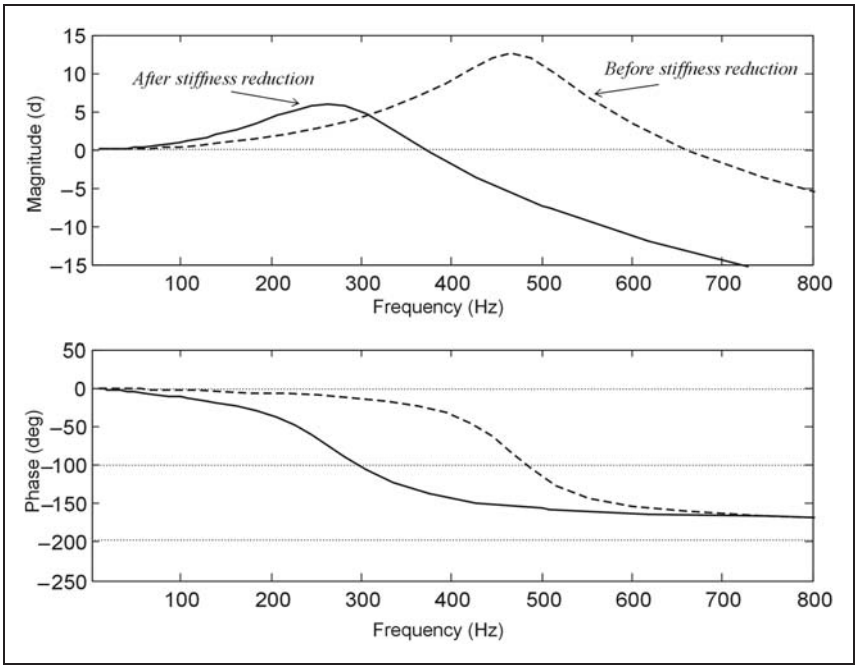

Figure 7. Predicted transmissibility from simulation results.

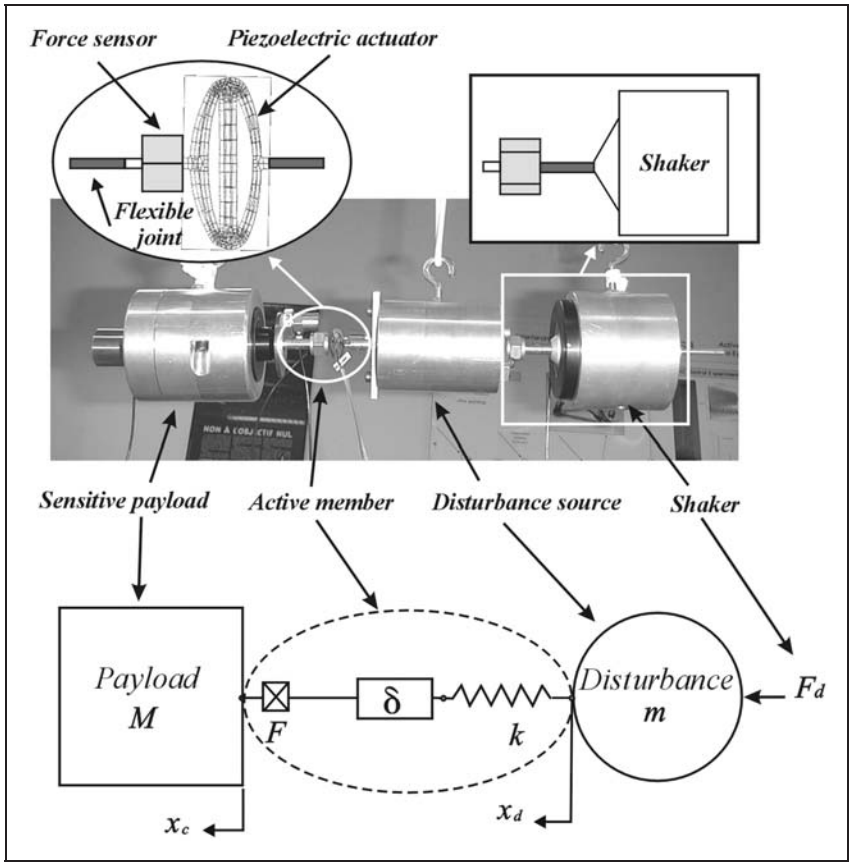

Figure 8. Experimental set-up of single axis piezoelectric isolator.

voltage signal. A high-pass filter at 1 Hz and a low-pass filter at 10 KHz have been applied, using the built-in filters in the charge amplifier, to limit the bandwidth of the system and to prevent the controller from the high frequency disturbing signals as well as from the low frequency wandering signal. From the output of the charge amplifier, the signal is acquired, converted to digital signal and fed into a PC digital signal processor (DSP) in which the PI compensator is built digitally. The filtered and compensated signal is converted to analog signal again to be taken out from the DSP output to the voltage amplifier and finally to the piezoelectric actuator which, in turn, acts against the measured vibration motion.

Using an external shaker, the system has been excited with a random signal ranging from 1 to 800 Hz and the transmissibility FRF between the displacement of the disturbance source body and that of the payload mass is measured. The resonance of the system is found at 500 Hz. A feedback system with a PI control law is applied to the system and the same FRF measured again. Figure 9 shows the two measured FRFs: the open-loop (before stiffness reduction) and the closed-loop (after stiffness reduction). The natural frequency of the system has been reduced 50%; from 500 Hz to 250 Hz. The maximum reduction has been obtained by increasing the gain of the proportional part of the compensator, but this leads to the risk of walking along the imaginary axis which can lead to instability if the surrounding conditions change slightly. Thus, there is a need to increase the integral gain too at the same time to increase the stability margin of the system and to reduce the overshoot in the resonance vicinity. Figure 10 shows a comparison between simulation and experimental results for the single axis vibration isolator. This figure shows the good matching between the two curves in open-loop before frequency reduction and in closed-loop after frequency reduction.

6. Mechanical truss structure

In the same context, another experiment has been done. The same control technique has been applied to the truss structure shown in Figure 11. The truss contains two active struts like the one shown in Figure 14 replacing two passive members. These two struts are used for the purpose of adding active damping to the system. The signals of the two force sensors, in the two active struts of the truss, have been filtered using the (PI) compensator in a DSP and fed back to the piezoelectric actuators.

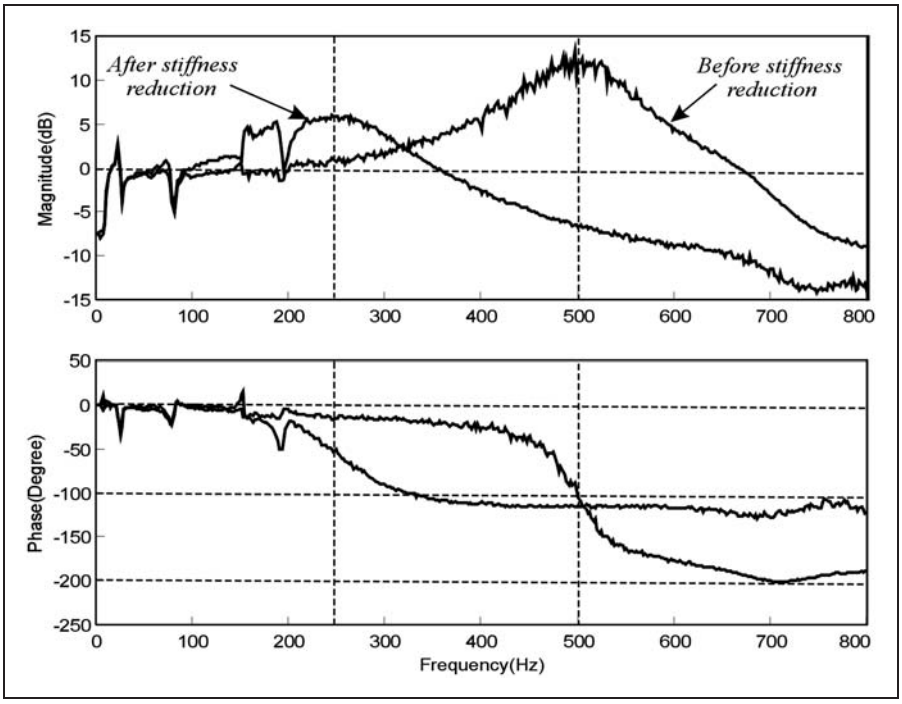

Figure 9. Experimental transmissibility (x_c/x_d).

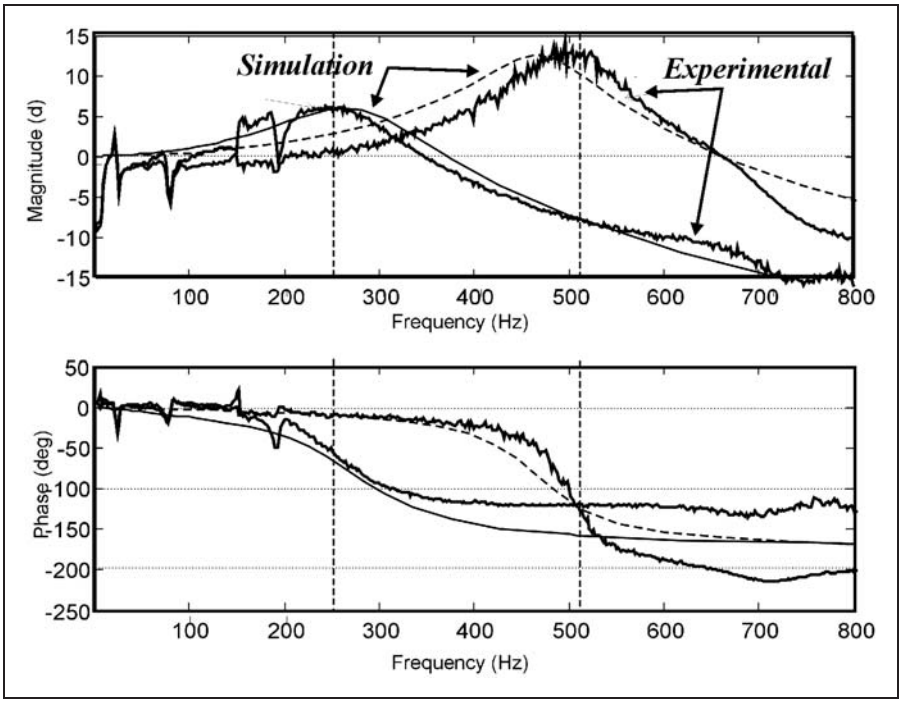

Figure 10. A comparison between simulation and experimental results.

The two control loops have been closed independently, forming a decentralized controller. Again, by increasing the proportional gain, the stiffness of the active struts in the structure has been reduced significantly. Figure 12 shows the first two modes of the FRF between the voltage input to one of the actuators and the force output from the collocated force sensor.The open-loop FRF (before stiffness reduction) shows that the two modes are located at 8.8 and 10.5 Hz. Using this control technique, they have been moved to 2.6 and

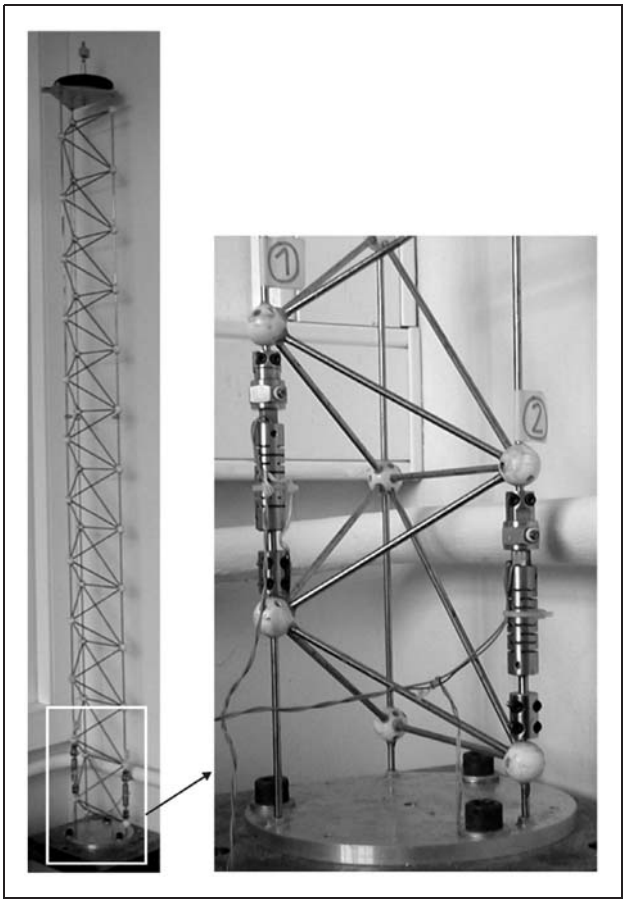

Figure 11. Passive mechanical truss with two active legs.

5 Hz, respectively. A potential application of this is the adaptation of structural resonances to a narrow band disturbance of variable frequency.

7. Six-axis stewart platform

Figure 13 shows a picture of the Université Libre de Bruxelles (ULB) piezoelectric Stewart platform; Figure 13(a) shows the complete Stewart platform where the connectors are the inputs to the actuators and the wires are the outputs of the sensors; Figure 13(b) shows the hexapod with the upper plate removed to show the details and configuration of the legs. The hexapod consists of two parallel plates connected to each other by six active legs. The legs are mounted in such a way to achieve the geometry of cubic configuration. Each active leg consists of a force sensor (B&K 8200), an amplified piezoelectric actuator (Cedrat APA50s) and two flexible joints as shown in Figure 14. In the ideal situation, the hexapod needs to be hinged using spherical joints, but to avoid the problem of friction and backlash, flexible tips are used instead of spherical joints. These flexible tips have the following properties: zero friction, zero backlash, high axial stiffness and relatively low bending stiffness. The bending stiffness of these joints makes a limitation for the active control authority, because it shifts the transmission zeros which decreases the closed-loop performance (Abu Hanieh et al., 2002; Preumont et al., 2002).

This interface has been used so far for the purposes of active damping and precision pointing only because

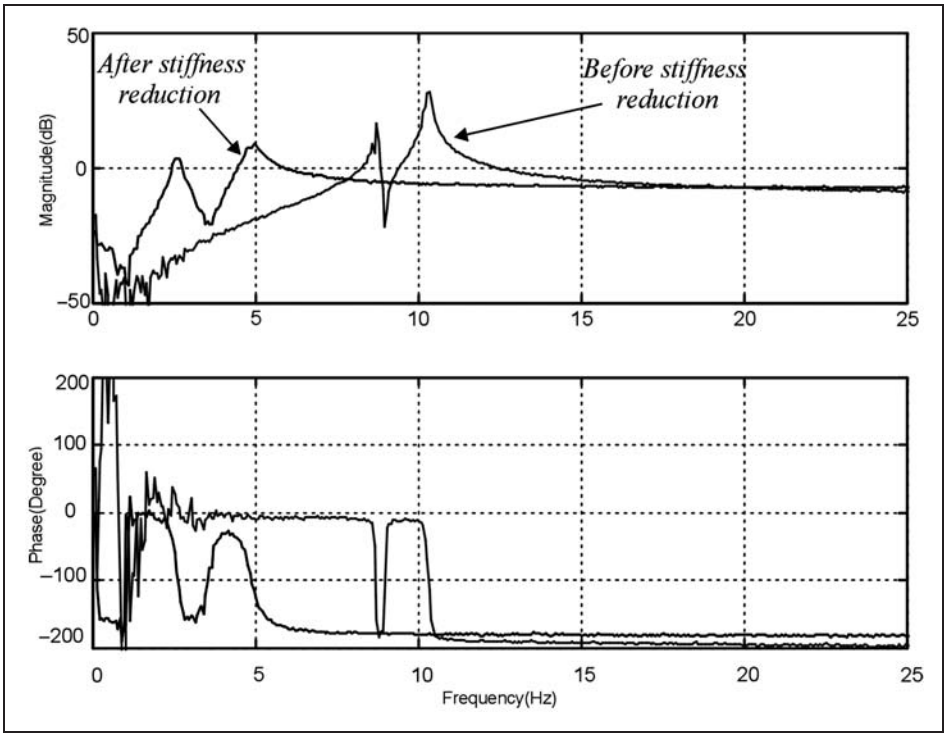

Figure 12. Experimental FRF between extension of the actuator and force in the leg.

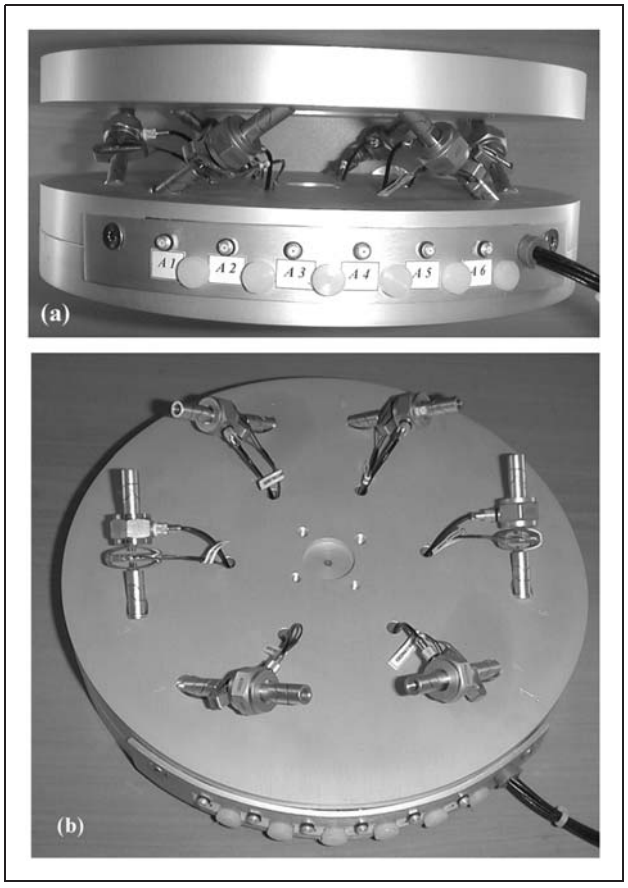

Figure 13. ULB stiff Stewart platform.

of high stiffness and rigidity in the legs. This six degrees-of-freedom interface can be used for active isolation of vibrations if the corner frequency of the interface is reduced and this can be done by the previously mentioned frequency reduction technique using PI controller.

The governing equation of motion in Laplace transform for the system is:

$$\mathbf{M}s^2x + \mathbf{K}x = \mathbf{Bk}\delta \tag{12}$$

where $\boldsymbol{M}$ is the mass matrix of the mobile platform, $\boldsymbol{K}$ is the stiffness matrix of the legs, $\boldsymbol{\delta}$ is the extension vector of the legs, $\boldsymbol{k}$ is the axial stiffness of the leg and $\boldsymbol{B}$ is the force Jacobian matrix that relates the six forces measured by the force sensors in the legs to the forces and torques of the mobile plate in the six degrees-of-freedom. Here, $\boldsymbol{k\delta}$ represents the force exerted by the piezoelectric actuator.

The sensor attached to the leg is the force sensor, this leads to the output equation:

$$\mathbf{y} = \mathbf{k}\left(\mathbf{B}^T x - \delta\right) \tag{13}$$

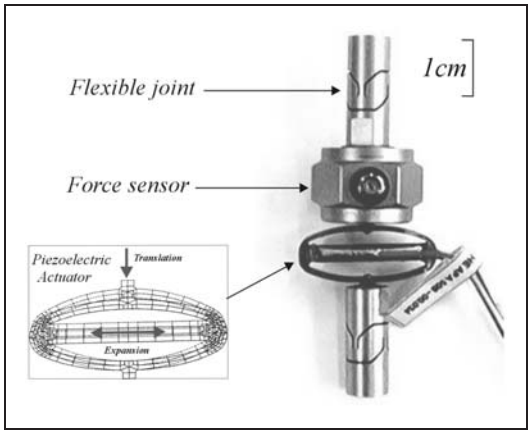

Figure 14. Active leg of the ULB stiff Stewart platform.

where $\boldsymbol{y}$ is a vector contains the six output readings of force sensors in the legs. The PI control equation reads:

$$\boldsymbol{\delta} = \frac{g}{\mathbf{k}s}(1 + as)\mathbf{y} \tag{14}$$

or

$$\boldsymbol{\delta} = \frac{g + gas}{1 + g + gas}\mathbf{B}^T x \tag{15}$$

This leads to the closed loop equation:

$$\left[\mathbf{M}s^2 + \mathbf{K} - \mathbf{BkB}^T\left(\frac{g + gas}{1 + g + gas}\right)\right]x = 0 \tag{16}$$

The previous equations show that increasing the proportional gain ga will subtract the second term from the stiffness which decreases the total stiffness of the system leading to reduce the natural frequency. While increasing the integration gain g leads to add some damping to the isolator increasing the stability of the control system.

8. Conclusions

The analytical, simulation and experimental result discussed in this paper prove clearly that frequency variation is a reasonable method that can be used in vibration isolation by reducing the corner frequency of the system. Another application for this method is to simultaneously escape from excitations by rapid changing. This is possible by using rapid piezoelectric actuators that are stiff enough to stand under loads and can be softened for the purpose of vibration isolation. A future work to be done on this method is to apply it experimentally on a multi function six degrees-of-freedom interface (Stewart platform). Simulation proved that the corner frequency can be reduced to low levels

but it was difficult to reach that level experimentally because of the misalignment of the experimental set-up that causes coupling with other exciting modes limiting the robustness and performance of the system.

References

Abu Hanieh A (2003) Active isolation and damping of vibrations via Stewart platform PhD thesis. Free University of Brussels, Brussels, pp. 100–104.

Abu Hanieh A, Horodinca M and Preumont A (2002) Six-degree-of-freedom parallel hexapods for active damping and active isolation of vibrations, *Journal de Physique IV* 12: 11–41.

Nelson P (1991) An active vibration isolation system for inertial reference and precision measurement, *Review of Scientific Instruments, American Institute of Physics* 62(9): 2068–2075.

Preumont A (2002) *Vibration Control of Active Structures*, 2nd edn. Kluwer Academic Publishers, Dordrecht, The Netherlands, pp. 113–121.

Preumont A, Francois A, Bossens F and Abu Hanieh A (2002) Force feedback vs. acceleration feedback in active vibration isolation, *Journal of Sound and Vibration* 257(4): 605–613.

TMC (2002) *Technical Background, Technical Report*. Technical Manufacturing Corporation, US Patent # 5,660,255 & 5,823,307 by Schubert et al., 26 August 1997.

Kaplow CE and Velman JR (1980) Active local vibration isolation applied to a flexible space telescope, *AIAA Journal of Guidance and Control* 3(3): 227–233.

Karnopp D and Trikha AK (1969) Comparative study of optimization techniques for shock and vibration isolation, *ASME Journal of Engineering for Industry* 91: 1128–1132.

Rahman Z, Spanos J and Blackwood G (1994) Active narrow band vibration isolation of large engineering structures, in *Proceedings of the First World Conference on Structural Control*, Pasadena, CA, 3–5 August 1994, paper 176.